

Modeling Platelet-Blood Flow Interaction Using Subcellular Element Langevin Method



Journal:	<i>Journal of the Royal Society Interface</i>
Manuscript ID:	rsif-2011-0180.R1
Article Type:	Research
Date Submitted by the Author:	n/a
Complete List of Authors:	Sweet, Chris; University of Notre Dame, Center for Research Computing Chatterjee, Santanu; University of Notre Dame, Department of Computer Science and Engineering Xu, Zhiliang; University of Notre Dame, Department of Applied and Computational Mathematics and Statistics Bisordi, Katharine; Indiana University School of Medicine, Department of Medical and Molecular Genetics Rosen, Elliot; Indiana University-Purdue University Indianapolis, Department of Medical and Molecular Genetics Alber, Mark; University of Notre Dame, Department of Applied and Computational Mathematics and Statistics
Subject:	Biocomplexity < CROSS-DISCIPLINARY SCIENCES, Biomathematics < CROSS-DISCIPLINARY SCIENCES, Computational biology < CROSS-DISCIPLINARY SCIENCES
Keywords:	platelet, blood clot, thrombus development, subcellular element model, computational biology, Langevin equation

SCHOLARONE™
Manuscripts

Modeling Platelet-Blood Flow Interaction Using Subcellular Element Langevin Method

BY CHRISTOPHER R. SWEET^{A,C,†}, SANTANU CHATTERJEE^B, ZHILIANG XU^A,
KATHARINE BISORDI^D, ELLIOT D. ROSEN^D, MARK ALBER^{A,†}

*A) Department of Applied and Computational Mathematics and Statistics,
University of Notre Dame, Notre Dame, IN 46556.*

*B) Department of Computer Science and Engineering, University of Notre Dame,
Notre Dame, IN 46556.*

*C) Center for Research Computing, University of Notre Dame, Notre Dame, IN
46556.*

*D) Department of Medical and Molecular Genetics, Indiana University School of
Medicine, Indianapolis, IN 46202.*

In this paper a new three-dimensional (3D) modeling approach is described for studying fluid-viscoelastic cell interaction, the Subcellular Element Langevin (SCEL) method, with cells modeled by Subcellular Elements (SCE) and SCE cells coupled with fluid flow and substrate models by using the Langevin equation. It is demonstrated that: 1) the new method is computationally efficient, scaling as $\mathcal{O}(N)$ for N SCEs; 2) cell geometry, stiffness and adhesivity can be modeled by directly relating parameters to experimentally measured values; 3) modeling the fluid-platelet interface as a surface leads to a very good correlation with experimentally observed platelet flow interactions. Using this method, the 3D motion of a viscoelastic platelet in a shear blood flow was simulated and compared with experiments on tracking platelets in a blood chamber. It is shown that the complex platelet flipping dynamics under linear shear flows can be accurately recovered with the SCEL model when compared to the experiments. All experimental details and supplementary information are archived at <http://biomath.math.nd.edu/scelsupplementaryinformation/>.

Keywords: I

Computational biology; platelet; cell-based subcellular element model; blood clot; thrombus development

1. Introduction.

Damage or inflammation of the blood vessel wall can lead to the development of an intravascular clot or thrombus. Venous thromboembolic disease is a significant biomedical problem with the annual incidence in the US being estimated as high as 900,000 cases per year leading to 300,000 deaths (Heit *et al.* 2005, Wakefield *et al.*

† Authors for correspondence: Mark Alber (malber@nd.edu) and Christopher R. Sweet (chris.sweet@nd.edu)

Article submitted to Royal Society

TeX Paper

2 Christopher R. Sweet^{a,c,†}, Santanu Chatterjee^b, Zhiliang Xu^a, Katharine Bisordi^d, Elliot D. Rosen^d, Mark Alber^{a,†}

2009). Understanding the processes involved in the formation and development of a thrombus is of significant biomedical importance.

The recruitment of platelets flowing freely in blood to sites of injury is a key step in the formation of a thrombus. Before contacting the vessel wall, free flowing platelets near the surface exhibit shear dependent flipping. The flipping of free flowing platelets affects the orientation of platelets when first contacting the surface of the vessel. After contact, platelet receptor component GPIb α of the GPIb-V-IX complex forms transient bonds with von Willebrand factor (vWF) exposed at the injury site. The rapid association and dissociation kinetics of the GPIb α -vWF results in transient tethering and subsequent flipping (or rolling) of platelets on the vessel surface (Laurence & Springer 1991, Savage *et al.* 1996). Interestingly, the formation of the GPIb α -vWF bond is influenced by the orientation of the platelet when contacting the surface. This GPIb α -vWF binding is critical for supporting the initial attachment (tethering) and subsequent translocation of platelets in flow (Cruz *et al.* 2000). The initial attachment permits other platelet receptors to interact with the ligands in the vessel wall and blood (GPIV - collagen, GPIaIIb with collagen and vWF) that in addition to contributing to adhesion also activate intracellular signaling pathways leading to platelet morphological changes and activation of another platelet receptor, GPIIb-IIIa, which is necessary for binding to fibrin(ogen), vWF, and vitronectin. These latter interactions are necessary for firm irreversible adhesion and the formation of stable platelet aggregates.

Therefore, several computational models have been developed to characterize platelet motion quantitatively and to study platelet-blood vessel wall adhesion dynamics. Image analysis of platelet motion in flow-chamber experiments was used in (Mody *et al.* 2005a) to identify motion of platelets before, during, and after contact with surface coated with vWF for a range of fluid shear stresses (0.2-0.8 dyn/cm²). An analytical two-dimensional model was also introduced in (Mody *et al.* 2005a) to characterize the flipping of tethered platelets. A three-dimensional computational model was presented in (Mody *et al.* 2005b, Mody *et al.* 2008a, Mody *et al.* 2008b) for simulating motion of platelet-shaped cell in a flow near a wall to elucidate GPIb α -vWF mediated platelet and substrate binding that leads to shear-induced platelet aggregation. The adhesion model, introduced in (King *et al.* 2001), was combined in (Mody *et al.* 2008a, Mody *et al.* 2008b) with the completed double layer-boundary integral equation method for solving Stokes hydrodynamics equation. Effects of hydrodynamics, the shape of platelets and proximity of a plane wall on cell-cell collisions and on two unactivated platelets bridged by GPIb α -vWF-GPIb α at high shear rates were investigated.

A number of methods modeling cells, cellular interactions and cell-flow interactions have been developed previously. The subcellular element (SCE) model introduced in (Sandersius & Newman 2008, Newman 2007) represents each cell by a collection of elastically coupled subcellular elements, interacting with each other via short-range potentials, and being dynamically updated using Langevin dynamics. Using a large number of subcellular elements, cells yield viscoelastic properties consistent with those measured experimentally. The cell-cell adhesion is modeled as a modified Morse pairwise potential. However, the SCE model in (Sandersius & Newman 2008, Newman 2007) does not couple the cell dynamics to that of the fluid. A parallel implementation of the subcellular element method for individual

Article submitted to Royal Society

1
2
3
4 cells residing in a lattice-free spatial environment is described in (Christley & Nie
5 2010) (without coupling to a flow).

6 The immersed boundary (IB) method (Peskin 1977, Peskin 2002) has been
7 widely used for modeling flexible structures immersed in a fluid. For instance, it was
8 applied to the study of blood flow around heart valves (Peskin & McQueen 1997).
9 The IB method of (Jadhav *et al.* 2005) represents a cell (leukocyte) as a massless
10 elastic membrane enclosing an incompressible fluid. The continuity between the
11 fluid and cell is achieved by the interpolation of the velocities from the fluid and
12 the distribution of the forces from the elastic membrane. An adhesion model em-
13 ployed in (Jadhav *et al.* 2005), represents individual receptor-ligand (P-selectin and
14 P-selectin-glycoprotein-ligand-1 pair) interactions as harmonic springs that form or
15 break according to probabilities depending on the values of forward and reverse
16 rate constants obtained from the literature (Dembo 1994). The immersed finite
17 element method (IFEM) (Liu *et al.* 2006) is similar to the IB method. However,
18 IFEM models a cell as an elastic solid with mass. A Lagrangian solid mesh for cells
19 moves on top of a fixed Eulerian fluid mesh which covers the entire computational
20 domain. Solutions in both the solid and the fluid subdomains are computed by the
21 finite element method and the continuity between the fluid and solid subdomains
22 is also enforced by the interpolation of the velocities and the distribution of the
23 forces with the reproducing Kernel particle method delta function. Cell-cell and
24 cell-vessel adhesion in (Liu *et al.* 2006) is modeled as a modified Morse pairwise
25 potential. In the papers (Fogelson & Guy 2004, Fogelson & Guy 2008) an IB based
26 method in which individual platelets were modeled as a massless elastic fiber, was
27 used to simulate the formation of platelet aggregates.

28 The Dissipative Particle Dynamics (DPD) method (Kojic *et al.* 2008, Pivkin &
29 Karniadakis 2008) is based on the idea of introducing discrete “soft” fluid parti-
30 cles to replace the continuum flow description. In addition to the “soft” particles,
31 random perturbations are introduced to model the fluid atoms interacting with
32 the immersed cellular structures, which are also modeled as collections of particles.
33 Many fine grained features of the fluid dynamics and immersed structures within
34 the fluid are often not resolved in detail. Additionally, the DPD method generally
35 requires many DPD particles in relation to the number of cells, which increases
36 computational cost. However, the work in (Pivkin & Karniadakis 2008) reveals the
37 potential to develop DPD based models with low computational cost for simulating
38 fluid and blood cell interactions.

39 Several models of thrombus formation have also been introduced, which take
40 the recruitment of free flowing blood cells and initial contact between blood cells
41 and blood vessel wall into account. For example, models (Fogelson & Guy 2004,
42 Fogelson & Guy 2008) used IB approach to study formation of platelet thrombi
43 in coronary-artery sized blood vessels. (Pivkin *et al.* 2006) developed a platelet
44 thrombi model using the force coupling method. In recent papers (Xu *et al.* 2008,
45 Xu *et al.* 2010, Xu *et al.* 2009a, Xu *et al.* 2010b, Mu *et al.* 2010, Mu *et al.* 2009) a
46 multi-scale model of venous thrombosis was introduced which combined continuum
47 sub-models for the blood flow and the chemical cascade, induced by tissue factors
48 at injuries, and discrete stochastic Cellular Potts Models (CPM) for simulating cell-
49 cell and cell-injury interactions. CPM has proven to be efficient in implementing
50 simulations of thousands of cells but has limited abilities in describing in detail cell
51 properties such as elasticity and shape.

52 *Article submitted to Royal Society*

1
2
3
4
5
6
7
8
9
10
11
12
13
14
15
16
17
18
19
20
21
22
23
24
25
26
27
28
29
30
31
32
33
34
35
36
37
38
39
40
41
42
43
44
45
46
47
48
49
50
51
52
53
54
55
56
57
58
59
60

4 Christopher R. Sweet^{a,c,†}, Santanu Chatterjee^b, Zhiliang Xu^a, Katharine Bisordi^d, Elliot D. Rosen^d, Mark Alber^{a,†}

In this paper we develop a new method for 3D flow-cell interaction simulations - the Subcellular Element Langevin (SCEL) method. This method uses SCE to simulate cell motion and deformation and the SCE cell is coupled to the plasma flow by a novel variation of the Langevin Equation (Skeel & Izaguirre 2002). The SCEL method allows one to model the mechanical properties of cells accurately, while retaining the $\mathcal{O}(N)$ computational scaling of Langevin solvers with short range interactions. It also confers greatly reduced computational cost. Our approach confers “forward” coupling between the flow field and the SCE.

We ran experiments on tracking motion of platelets in a blood flow chamber. Human platelets were introduced into a plasma flow passing through a rectangular capillary tube. Images were captured at a rate of 30 fps and individual platelets were tracked for analysis. Flipping of the platelets was detected by measuring the minor and major axes of the platelets in each frame, since the shape of a platelet is approximately elliptical in cross section with the ratio of minor and major axes being 0.5 and the diameter of the platelet being $4\ \mu\text{m}$. The angle of the platelet then was deduced and the time to complete a flip was calculated.

It is demonstrated in this paper that: 1) the new Subcellular Element Langevin (SCEL) method is computationally efficient, scaling as $\mathcal{O}(N)$ for N SCEs; 2) cell geometry, stiffness and adhesivity can be modeled by directly relating parameters to experimentally measured values; 3) modeling the fluid-platelet interface as a surface leads to a good correlation with experimentally observed platelet flow interactions. Using this method, the 3D motion of a viscoelastic platelet in a shear blood flow was simulated and compared with experiments on tracking platelets in a blood chamber. It is shown that the complex platelet flipping dynamics under linear shear flows can be accurately recovered with the SCEL model when compared to the experiments.

The paper is organized as follows. Section 2 describes in detail SCE cell-based model coupled to the flow by utilizing a novel variation to the Langevin Equation. Section 3 describes simulations of flipping platelet moving in a linear shear flow and refines the choice of parameter values used in simulations. Section 4 includes conclusions and discussion of the future work. Section B.1 of the Supplementary Material discusses the numerical schemes to solve model equations. Biological Background Section in the Supplementary Material provides biological details about platelet and blood interaction.

2. Model description

In what follows we describe a new method for 3D flow-cell-wall interaction simulations, the Subcellular Element Langevin (SCEL) method. This method utilizes SCE to model the cells and the Langevin equation is employed to couple the SCE to the plasma flow.

This coupling idea is similar to the DPD extension in that the microscopic fluid-SCE interactions can be modeled (as random forces) and that the fluid acts as a heat bath. We extend the Langevin equation to allow the coupling of the coarser flow structure using a Stokes-Langevin approach (Skeel & Izaguirre 2002). Perturbations in the flow field at the cellular scale are assumed to couple to SCE using Stokes' law, with the force being proportional to the fluid velocity.

Article submitted to Royal Society

(a) *Model assumptions*

We assume that the plasma-cell mixture is homogenous up to cells attached to the injury site or rolling on the substrate surface. We assume that in a free-flowing environment the cells will eventually achieve the same velocity as the underlying fluid, moving cells do not affect the flow as we only consider the “forward coupling” in the present paper. The fluctuation-dissipation theorem assumes that the random forces can be positive or negative with equal probability (Gardiner 2004), an assumption which may be violated by the introduction of a biased flow. To reduce such errors we subtract the average flow velocity from the system (combined plasma and SCE) velocity for propagation of the SCE and assume, since the flow is considered incompressible, that the resulting flow field is un-biased.

(b) *Subcellular elements and forces*

Our coarse grained approach is based on modeling the platelets and blood cells using subcellular elements (SCE) and treating the solvent (plasma) as removed degrees of freedom that are introduced stochastically as velocity damping and random fluctuation.

(i) *Subcellular Element Model of cells and schematic of problems being modeled*

Newman *et al.* introduced the Subcellular Element model (Sandersius & Newman 2008, Newman 2007) to compute the dynamics of large number of three-dimensional deformable cells in multicellular systems. In the SCE model framework, each cell is represented by a collection of elastically linked subcellular elements, interacting with one another via short-range potentials. Figure 1(b) shows SCE representation of a platelet in our model. In our cell representation, a cell composes of a subcellular element at the cell center and a set of subcellular elements discretizing the proximity of surface of the cell (discussed in Section ii). The position of a subcellular element changes according to three processes (or forces): (1) a stochastic component simulating cellular fluctuation; (2) an elastic force by intra-cellular interactions; (3) a hydrodynamic force by fluid-cell interaction. To this end, the a modified Langevin equation including these three processes are utilized to update the position of a subcellular element. Using this model, we simulate the platelet motion by placing the platelet in a linear shear flow field within a rectangular channel.

(ii) *Cell mechanical properties*

Each cell consists of a number of surface nodes (or SCEs) and a central node (or a central SCE). The surface nodes represent points close to the cell surface (defined below) and the central node represents a point close to the cell nucleus. The mechanical properties and geometry of a cell are modeled by connecting each surface node to both its immediate neighbors and the central node, by harmonic “spring” forces of given rest length. The associated potential energy function for bodies i and j are

$$U_{ij}^e = \frac{k_{ij}}{2} (|\mathbf{r}_{ij}| - l_{ij})^2, \quad (2.1)$$

Article submitted to Royal Society

6 Christopher R. Sweet^{a,c,†}, Santanu Chatterjee^b, Zhiliang Xu^a, Katharine Bisordi^d, Elliot D. Rosen^d, Mark Alber^{a,†}

where l_{ij} is the rest length, $\mathbf{r}_{ij} = \mathbf{x}_j - \mathbf{x}_i$ the position vector difference for bodies i and j respectively and k_{ij} the coefficient that defines the spring “stiffness”. The corresponding force vector acting on body i by body j is

$$\mathbf{F}_{ij}^e = -\nabla_{\mathbf{x}} U_{ij}^e(\mathbf{x}) = -k_{ij}(\|\mathbf{r}_{ij}\| - l_{ij})\hat{\mathbf{r}}_{ij}, \quad (2.2)$$

here $\hat{\mathbf{r}}_{ij}$ is a unit vector defined by $\hat{\mathbf{r}}_{ij} = \frac{\mathbf{r}_{ij}}{\|\mathbf{r}_{ij}\|}$.

We note that the effective surface of a SCE cell is defined by the intersection of the spheres of radius σ around each node. σ is dependent on the SCE geometry and should be chosen to give a continuous platelet surface i.e. its diameter should be greater than the distance between adjacent SCEs. A detailed description of the choice of σ can be found in Section 3i.

(iii) Cell-Vessel wall interaction

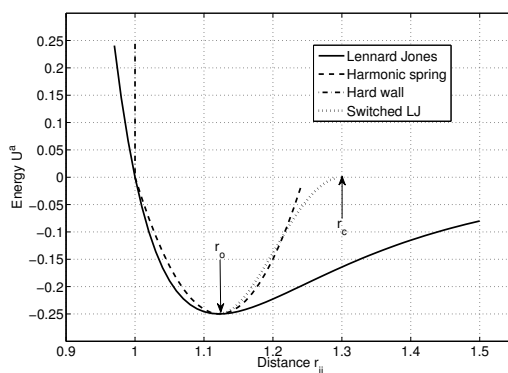
Previous attempts to resolve SCE cell-substrate interactions have used a simplistic pairwise interaction based on the Morse potential (Sandersius & Newman 2008, Newman 2007). We have extended the SCE model to prevent cellular-vessel overlap and also to allow accurate representations of cell rolling dynamics. This has been accomplished by using the idea of bonds, representing ligand-receptor (GPIb α -vWF in our case) pairs, that break beyond a given extension (Jadhav *et al.* 2005, Krasik *et al.* 2006, Mody & King 2008b). Since the number of SCEs representing a cell is generally much less than the number of platelet receptor sites, the statistics of modeling many ligand-receptor pairs per SCE is well defined.

The ligand-receptor adhesion modeling component in our model is an extension of the original SCE Morse pairwise potential (Newman 2007). Namely, we integrate an adhesion submodel from (Krasik *et al.* 2006) into the SCE model (We note that similar adhesion models were used in (Jadhav *et al.* 2005, Mody & King 2008b) for the study of selectin-mediated leukocyte rolling and platelet-platelet bridging by forming GPIb α -vWF-GPIb α bonds respectively. However, in those works, the bond force is directly calculated.). In the work of (Krasik *et al.* 2006), the adhesion model was developed to study the mechanisms of the neutrophil arrest. Here the probabilities of breakage and formation of bonds are calculated using the Bell model (Bell 1978).

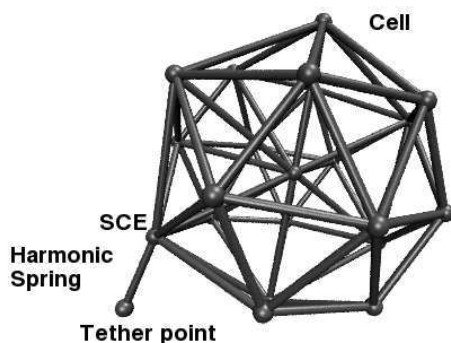
Our approach to modeling platelet adhesivity is to introduce forces representing the observed receptor-ligand interactions *averaged* over the individual SCE surfaces, and to model their stochastic behavior via the Langevin equation. We introduce individual linear springs between each of the SCE and the vessel wall to mimic the receptor-ligand interactions. Parameters in the cell-wall interaction model are determined by the mechanical properties of the receptor-ligand bond, the number of such bonds that are likely to form, given cell contact surface area, and the probability of the bonds breaking beyond a given length (Jadhav *et al.* 2005, Krasik *et al.* 2006, Mody & King 2008b). Each SCE/vessel wall interaction is represented by a potential energy function, which is a quadratic function truncated at the maximum and minimum length of the spring (bond) (see Figure 1(a) dashed line). To prevent the SCE surface and the vessel wall from overlapping, a “hard wall” interaction term is added (Hansen & McDonald 1986) (see Figure 1(a) the vertical (dash-dot) line).

Article submitted to Royal Society

Since forces in our model are defined as the negative of the gradient of the potential energy, we have to modify this function so that it is continuous, i.e. the spring (bond) cannot break instantaneously. Our approach is illustrated in Figure 1(a). The ideal force which combines harmonic spring force and “hard wall” force, prevents overlap between the SCE (on the cell surface) and the substrate. We approximate this force with a pairwise potential (PP) of the Lennard-Jones type (Lennard-Jones 1924, Frenkel *et al.* 2002) that emulates the “hard wall” and the first section of the spring potential well. Since the PP force has a long “tail” we truncate this by using a “switch” which turns off the PP force over a short distance and prevents instantaneous energy changes. The result is a non-linear spring with a known region of breakage coupled to the defined surfaces that cannot overlap.



(a) Potential energy U^a change with inter SCE distance r_{ij} showing switch on point r_o and switch cutoff r_c .



(b) Harmonic tether.

Figure 1. Cell-Substrate interaction potential energy.

8 Christopher R. Sweet^{a,c,†}, Santanu Chatterjee^b, Zhiliang Xu^a, Katharine Bisordi^d, Elliot D. Rosen^d, Mark Alber^{a,†}

The potential energy function between the SCE i and the substrate point j is

$$U_{ij}^a = \epsilon_{ij} \left(\left(\frac{\sigma_{ij}}{r_{ij}} \right)^{12} - \left(\frac{\sigma_{ij}}{r_{ij}} \right)^6 \right) S(r_{ij}), \quad (2.3)$$

where $\mathbf{r}_{ij} = \mathbf{x}_j - \mathbf{x}_i$ is the SCE-substrate vector and $r_{ij} = \|\mathbf{r}_{ij}\|$. ϵ_{ij} and σ_{ij} define the adhesion level and distance respectively. The switch S is defined as

$$S(r_{ij}) = \begin{cases} 1 & \text{if } r_{ij} \leq r_o, \\ \frac{(r_{ij}^2 - r_c^2)^2 (r_c^2 + 2r_{ij}^2 - 3r_o^2)}{(r_o^2 - r_o^2)^3} & \text{if } r_o \leq r_{ij} < r_c, \\ 0 & \text{if } r_{ij} > r_c, \end{cases} \quad (2.4)$$

where r_o is the switch-on value and r_c is the cutoff value.

The corresponding vector acting on the SCE i is

$$\mathbf{F}_{ij}^a = - \left(\frac{dU_{ij}^a(r_{ij})}{dr_{ij}} S(r_{ij}) + \frac{dS(r_{ij})}{dr_{ij}} U_{ij}^a(r_{ij}) \right) \hat{\mathbf{r}}_{ij}. \quad (2.5)$$

Having defined the form of the potential energy we now need to determine the position of the substrate point j . We assume that the substrate surface consists of discrete contact points with a known ‘granularity’. The point nearest to the SCE i on the substrate is calculated (using the normal to the substrate surface) and the nearest discrete point, in a direction opposite to the SCE velocity, is selected. Specifically, given a unit vector normal to a plane tangential to the substrate (blood vessel wall) $\hat{\mathbf{n}}_p$ and point on this plane \mathbf{x}_p . We find the distance to the plane $\Delta d = \hat{\mathbf{n}}_p \cdot (\mathbf{x}_i - \mathbf{x}_p)$. We then find the ‘anchor’ point

$$\mathbf{x}_j = \mathbf{x}_i + \Delta d \hat{\mathbf{n}}_p - \frac{\mathbf{v}'_i}{\|\mathbf{v}'_i\|} \Delta g, \quad (2.6)$$

for granularity Δg and vector \mathbf{v}'_i , the i^{th} SCEs velocity projected onto the plane. The granularity Δg represents the average distance between receptor-ligand on the substrate.

To parameterize Eqns. (2.3)-(2.4) we need to find the spring constant associated with extending the combined microvillus and receptor-ligand k_s , the rest length (un-forced) length d_{rest} and breaking length $d_{\text{rest}} + \delta d$ of the combined microvillus and receptor-ligand. The parameters σ_{ij} , ϵ_{ij} are then derived from these. Given the required spring constant k_s , receptor-ligand rest length d_{rest} and breaking extension δd , we can calculate the variables ϵ_{ij} , σ_{ij} , switch on distance r_o and switch cutoff r_c from Eqns. (2.3)-(2.4)

$$\sigma_{ij} = 2^{-\frac{1}{6}} d_{\text{rest}}, \quad (2.7)$$

$$\epsilon_{ij} = 4k_s (\delta d)^2, \quad (2.8)$$

$$r_o = d_{\text{rest}}, \quad (2.9)$$

$$r_c = d_{\text{rest}} + \delta d. \quad (2.10)$$

Since there is no experimental data for the platelet GPIb α receptor and the wall immobilized vWF ligand binding bonds, we assume that the mechanical properties

Article submitted to Royal Society

of the platelet-wall binding bonds are similar to these of the leukocyte selectin-ligand bonds. Therefore spring constants, receptor-ligand rest length and breaking extension distances are taken from (Jadhav *et al.* 2005).

A discussion of the parameterization can be found in the Results Section. The SCEL simulation work flow can be seen in Figure 2. The platelet geometry and force parameters for the simulation are generated using the SCE factory written in Python. The resulting simulation files are input to the SCEL simulation engine to produce the relevant trajectory files. The platelet angles are then extracted from the trajectory files are then using Matlab scripts which are available on the supplementary information website.

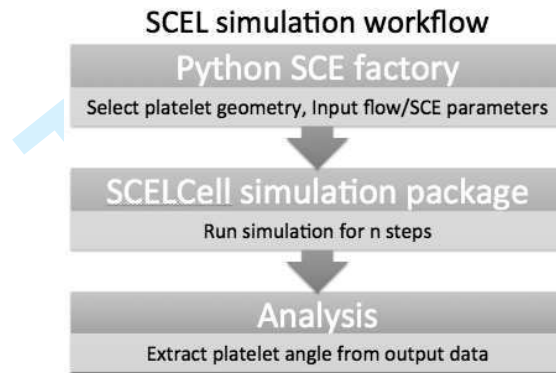


Figure 2. Cell-Substrate interaction potential energy.

(iv) *Brownian dynamics*

The simplest fluid-SCE interaction can be modeled as Brownian dynamics. Consider a body with mass m and radius r moving with velocity v in a fluid with viscosity η . The fluid effectively applies a force f to the body in the opposite direction to its movement, which we typically approximate with $f = -\gamma v$ for friction coefficient γ . We can calculate γ from Stokes' law $\gamma = 6\pi\eta r$. The simplistic equation of motion is then

$$m \frac{dv}{dt} = -\gamma v, \quad (2.11)$$

with solution

$$v(t) = e^{-\gamma t/m} v(0). \quad (2.12)$$

Clearly the velocity would go to zero as time increases, which is not what we observe in reality. We can improve the model by simulating the, assumed random, collisions of the fluid particles with the body. The equation of the motion now becomes

$$m \frac{dv}{dt} = -\gamma v + \delta R(t), \quad (2.13)$$

for the random force $\delta R(t)$. We make the following assumptions about $\delta R(t)$ by considering that the sum effect of the collisions must be unbiased and that the

10 Christopher R. Sweet^{a,c,†}, Santanu Chatterjee^b, Zhiliang Xu^a, Katharine Bisordi^d, Elliot D. Rosen^d, Mark Alber^{a,†}

force of the impacts varies extremely rapidly in any infinitesimal time interval

$$\langle \delta R(t) \rangle = 0, \quad \langle \delta R(t) \delta R(t') \rangle = S \delta(t - t'), \quad (2.14)$$

for S being the strength of the random force.

Assuming that the fluid acts as a constant temperature “heat-bath” we have

$$\left\langle \frac{1}{2} m v^2 \right\rangle = \frac{N k T}{2}, \quad (2.15)$$

for N being the degrees of freedom (d.o.f.), k the Boltzmann coefficient and T the temperature.

From Eqns. (2.14)-(2.15) we can show that $\delta R(t)$ is satisfied by a random variable with a Gaussian distribution, zero mean and variance of $2\gamma k T$. Before we discuss our approach to modeling fluid-SCE interaction, we would like to point out that Brownian motion of a platelet in the creeping flow regime near a surface has been studied in (Mody *et al.* 2007) indicating that Brownian motion played an insignificant role in influencing platelet motion.

(v) *The Langevin equation*

The more complex scenarios of the fluid-SCE interaction can be modeled by using the Langevin equation, allowing the introduction of systematic forces related to SCEs. Given a system of N bodies with a potential energy $U(\mathbf{x})$ as a function of position vector \mathbf{x} , then conservative force vector is given by the gradient $\mathbf{F}(\mathbf{x}) = -\nabla U(\mathbf{x})$ and our equation of the motion becomes

$$\mathbf{M} \ddot{\mathbf{x}} = \mathbf{F}(\mathbf{x}) - \gamma \dot{\mathbf{x}} + \sqrt{2\gamma N k T} \mathbf{Z}, \quad (2.16)$$

where \mathbf{Z} is a vector of normally distributed random variables and \mathbf{M} is the diagonal matrix of particle masses.

More rigorous analysis of the method can be made by considering Mori-Zwanzig formalism, and making the appropriate model dependent approximations. This is the basis for many coarse-grained methods, generally a new set of variables is chosen to model “important” aspects of the system (usually slow d.o.f.) and the remaining d.o.f. (usually fast and in our case the fluid) are modeled by their effects on the chosen variables.

Given the large scale separation of the model we require a numerical propagation method that gives the correct solutions for large time step Δt and damping coefficient γ . Appropriate methods that give the correct solution for $\gamma \Delta t \gg 1$ (Izaguire *et al.* 2010) are discussed in Numerical Methods Section in Supplementary Material.

(vi) *Coupling technique*

Our problem is to model the interactions of a *flowing* fluid with bodies representing the blood cellular constituents. This is an extension to the general idea of non-equilibrium system, which are generally close to equilibrium in some sense. For instance the expected value of the kinetic energy per degree of freedom is now not equal to $kT/2$.

Article submitted to Royal Society

The flow is calculated on a 3D grid where the distance between the grid points, Δd , is similar to the platelet dimensions of $2\text{-}4\mu\text{m}$. The grid is defined on a domain with $x \in [0, X]$, $y \in [0, Y]$, $z \in [0, Z]$. We define the fluid velocity vector at grid point i, j, k to be \mathbf{v}_{ijk}^g with corresponding position $\mathbf{g}_{ijk} = \{i\Delta d - \frac{\Delta d}{2}, j\Delta d - \frac{\Delta d}{2}, k\Delta d - \frac{\Delta d}{2}\}$, with the indices bounded by $I = \frac{X}{\Delta d}$, $J = \frac{Y}{\Delta d}$, $K = \frac{Z}{\Delta d}$ for i, j and k respectively. The flow is incompressible, so is divergence free. Hence for a given constant inlet velocity we have a well defined average 3D velocity vector

$$\langle \mathbf{v}^f \rangle = \frac{1}{IJK} \sum_{i=1}^I \sum_{j=1}^J \sum_{k=1}^K \mathbf{v}_{ijk}^g. \quad (2.17)$$

We define the flow velocity at SCE m as

$$\mathbf{v}_m^f = \mathbf{v}_{abc}^g \text{ where } \{abc\} = \arg \min_{i,j,k} \|\mathbf{x}_m - \mathbf{g}_{ijk}\|. \quad (2.18)$$

The system flow velocity vector for inclusion in the modified Langevin framework is then $\mathbf{v}^f = [\mathbf{v}_1^f, \dots, \mathbf{v}_N^f]^T$.

We consider the dynamics to be in a reference frame having velocity $\langle \mathbf{v}^f \rangle$. We then need to consider the interaction between the underlying flow perturbation vector $\delta \mathbf{v}^f = \mathbf{v}^f - \langle \mathbf{v}^f \rangle$ with the bodies of interest. The additional force vector \mathbf{f}^f on the bodies can again be modeled by using Stokes' law, which gives $\mathbf{f}^f = \gamma \delta \mathbf{v}^f$.

Then we have

$$\mathbf{M} \dot{\mathbf{x}} = \mathbf{F}(\mathbf{x}) - \gamma (\dot{\mathbf{x}} - \delta \mathbf{v}^f) + \sqrt{2\gamma NkT} \mathbf{Z}. \quad (2.19)$$

Note that we need to add the average velocities to those resulting from these equations to get the observed velocities \mathbf{v}_o . i.e.

$$\mathbf{v}_o = \dot{\mathbf{x}} + \langle \mathbf{v}^f \rangle, \quad (2.20)$$

and add the average movement of the reference frame to get the observed positions \mathbf{x}_o

$$\mathbf{x}_o = \mathbf{x} + \Delta t \langle \mathbf{v}^f \rangle. \quad (2.21)$$

(vii) *Surface interface modification*

Eqn. (2.19) does not take account of the cellular surface, each SCE is treated as if it is immersed in the fluid. A more realistic interaction can be achieved by scaling the damping factor γ along the vector connecting the surface SCE to the SCE at the cell center. We denote this "surface interface" modification as SIM. The center SCE should see no effect from the flow. The damping applied to SCE i , given local damping factor γ_i is

$$\gamma_i = \begin{cases} s_i \gamma & s_i > 0, i \notin \Phi, \\ \mathbf{0} & s_i \leq 0, \\ \mathbf{0} & i \in \Phi, \end{cases} \quad (2.22)$$

where Φ is the set of SCE not on the cell surface and

$$s_i = \begin{cases} \frac{\delta \mathbf{v}_i^f \cdot \mathbf{sc}_i}{\|\delta \mathbf{v}_i^f\| \|\mathbf{sc}_i\|} & \delta \mathbf{v}_i^f \neq \mathbf{0}, \\ 0 & \delta \mathbf{v}_i^f = \mathbf{0}, \end{cases} \quad (2.23)$$

Article submitted to Royal Society

12 Christopher R. Sweet^{a,c,†}, Santanu Chatterjee^b, Zhiliang Xu^a, Katharine Bisordi^d, Elliot D. Rosen^d, Mark Alber^{a,†}

here $\mathbf{sc}_i = \mathbf{x}_i - \mathbf{x}_c$, and \mathbf{x}_c is the position of the SCE at the center of the cell associated with SCE i .

The updated equation is

$$\mathbf{M}\ddot{\mathbf{x}} = \mathbf{F}(\mathbf{x}) - \Gamma(\dot{\mathbf{x}} - \delta\mathbf{v}^f) + \sqrt{2NkT} \Gamma^{\frac{1}{2}} \mathbf{Z}, \quad (2.24)$$

where Γ is now a matrix containing the γ_i .

3. Results

We tested whether our model provides accurate fluid mechanical solutions that can be applied to microscopic spherical and ellipsoidal cells in a bounded fluid. We note that any shapes of cells can be represented by the model. To validate our method we compare with both theoretical studies and actual experiments of platelets flipping in the plasma flowing through a capillary tube. We separate the results into comparisons with theoretical and experimental results respectively. All experimental details and supplementary information are archived at <http://biomath.math.nd.edu/scelsupplementaryinformation/>.

Figure 5 shows the snapshots of the platelet during the flipping process in our simulations.

(a) Comparison with experimental data

Here we compare the experimental results of flipping platelets conducted *in vitro* with the simulation results. We show that we have achieved good agreement between experiments and simulations.

(i) Experimental and simulation conditions

Flipping of the platelets is detected by measuring the minor and major axes of the platelets in each frame, since the shape of a platelet is approximately elliptical in cross section with $\lambda = 0.5$ with the diameter of the platelet being $4 \mu\text{m}$. The angle of the platelet can then be deduced and the time to complete a flip can be calculated.

The motion of platelets in different experiments was measured in a platelet rich plasma prepared from ACD anticoagulated blood from the same healthy donor after informed consent on different days. The platelet counts in the blood samples were in the normal range 2.2 to $2.5 \times 10^5/\mu\text{l}$.

Two separate sets of experiments were carried out, differing in the flow rate of $4 \mu\text{l min}^{-1}$ or $10 \mu\text{l min}^{-1}$ and also the date on which the platelets were obtained (from the same subject). Platelet rich plasma was drawn through a $0.2 \times 2.0 \text{ mm}$ rectangular capillary tubes (Vitricon, NJ) at $4 \mu\text{l/min}$ or $10 \mu\text{l/min}$. The motion of flowing platelets was recorded by videomicroscopy at 30 fps. Each experiment enabled one to follow multiple different platelets. In the first experiment the average flow velocity through the capillary was 0.1667 mm s^{-1} and the maximum platelet velocity was estimated to be 0.4 mm s^{-1} . In the second experiment the average flow velocity through the capillary was 0.4168 mm s^{-1} and the maximum velocity was estimated to be 0.7 mm s^{-1} .

Article submitted to Royal Society

To estimate the shear we assume that the velocity profile is parabolic with zero velocity at the wall of the capillary tube and the maximum platelet velocity is estimated by finding the platelet with the highest velocity. The shear rate ζ for a platelet can then be readily calculated and, with the observed flipping time t , the product $t\zeta$ can be found (see also experimental results section for these estimated values).

In the first experiment ten platelets, with velocities ranging from 0.08-0.13 mm s⁻¹ were measured and the upper and lower bounds were found for the flipping time-shear rate products.

In the second experiment a further twelve platelets, with velocities ranging from 0.08-0.39 mm s⁻¹ were measured and again the upper and lower bounds were found for the flipping time-shear rate products.

The simulations were repeated with a platelet of diameter of 4 μ m and $\lambda = 0.5$ (c.f. 2 μ m and $\lambda = 0.25$ in the theoretical experiments above).

(ii) *Experimental results*

Frames from the first set of experiment for one flipping platelet can be seen in Figure 3. Frames 8, 11, 13 and 16 from the file “Grabbed Frames from 7-8-2010 4ul-min 2mm cap PRP + Ca.ppt” in the supplementary material and the calibration grid (for converting pixel measurements from the camera frames to physical measurements) has graduations of 10 μ m. The platelet can be seen to transition from an elliptical cross-section in Frame 1 to circular in Frame 3 and back to elliptical in Frame 4. This represents a half flip (through 180 degrees) in 7 frames (233 ms at 30 fps), which has a velocity of 0.17 mm s⁻¹, and a shear rate (from the parabolic profile assumption) of 6.7 s⁻¹. The time-shear rate product is 1.58 (unit-less). We would like to remark that this shear rate is quite low compared to physiological values in the circulation or in previous platelet studies (Mody *et al.* 2005a), by two orders of magnitude. The microfluidic experimental system utilized in the study required low flow rates in order to capture high resolution images of flipping platelets. However, this value of shear rate does not invalidate any of the analysis conducted in the paper.

The results for the two sets of experiments can be found in Table 1. The average $t\zeta$ product for each experiment are close in value, we note that the Standard Deviation (SD) for $t\zeta$ is larger at the higher velocity. Complete tabular data for these experiments can be found in the supplementary information.

The average time-shear rate product for each experiment set, plotted with the simulation results in Figure 4, show good correlation. Here the solid curve represents the simulation results and the dotted lines show the mean and 1 SD for each of the experiment sets, showing small error in the simulation. The simulation method reproduces the flow interacting with the human platelets with an observed maximum error (difference in flipping time of experiment and simulation normalized by the simulation flipping time) of less than 2 SD for the first experimental set and less than 1 SD for the second experimental set.

Article submitted to Royal Society

14 Christopher R. Sweet^{a,c,†}, Santanu Chatterjee^b, Zhiliang Xu^a, Katharine Bisordi^d, Elliot D. Rosen^d, Mark Alber^{a,†}

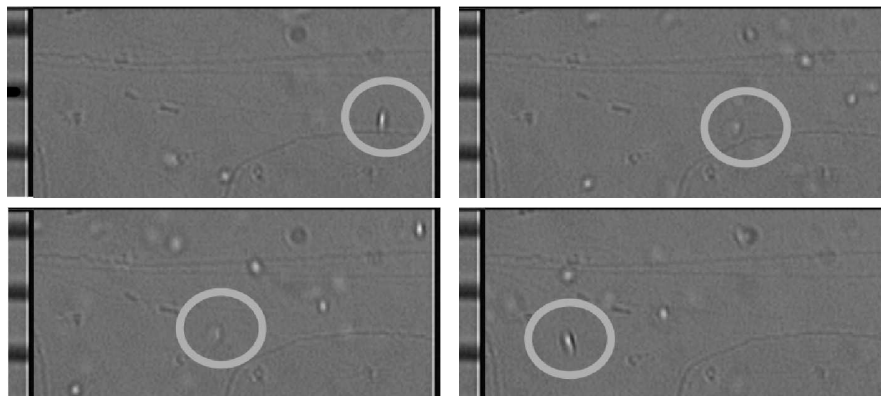


Figure 3. Experimentally observed flipping of a human platelet traveling from right to left. The calibration grid has graduations of $10\ \mu\text{m}$. Snapshots taken from frames 8, 11, 13 and 14 from the file “Grabbed Frames from 7-8-2010 4ul-min 2mm cap PRP + Ca.ppt” in supplementary information.

Table 1. Platelet flipping results

Experiment set	Flow $\mu\text{l min}^{-1}$	Average $t\zeta$	Standard deviation $t\zeta$
1	4	1.6556	0.0814
2	10	1.6972	0.3553
Simulation	-	1.81	-

(b) Comparison to theoretical studies

We compare in what follows our simulation results with the results of (Mody & King 2005a), which describes theoretical solutions obtained using Jeffery orbit theory (G. B. Jeffery 1922) and provides predictions obtained using analytic platelet flipping model.

Specifically, we compared our simulation predictions of the effect of the wall on the rotational motion of a platelet where the ratio of major and minor axes are $\lambda=0.25$ and $\lambda=0.5$ with the analytical solutions for a circular disk computed by (Kim et al. 1997). The platelet or circular disk was oriented with its major axis parallel to the surface so that its axis of symmetry lay at right angles to the surface, see Figure 5. These results are verified using the analytical solutions of (G. B. Jeffery 1922) for the rotational trajectory of an oblate spheroid flowing in the linear shear flow in an unbounded fluid.

In addition to the basic Langevin-Stokes coupling, we have introduced the “surface interaction” (SIM) method in Section vii as an extension to the Langevin-Stokes idea. We illustrate the effects of this modification in the tests as well.

(i) Modeling parameters

For modeling the platelet dynamics we use a set of units based on distance in μm , mass in μg and time in μs .

Article submitted to Royal Society

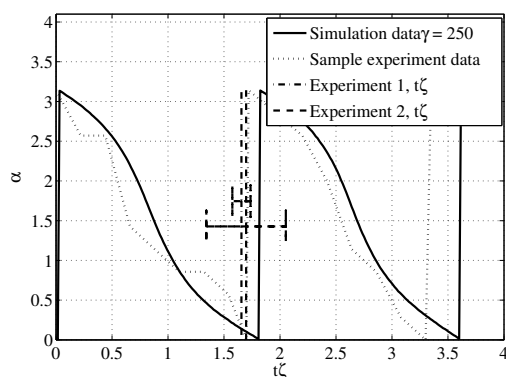


Figure 4. Comparison of the simulated platelet flipping dynamics with the experiment results for human platelets. The solid curve represents the simulation and the dark-dashed curves represent the results from experiment sets 1 and 2 with error bars at 1 SD. Both showing good correlation with the simulated flipping times. The light-dotted curve represents the actual measured angle of the representative platelet. The variation in angle α to the platelet major axis is plotted against the unit-less time, shear-rate product $t\zeta$.



Figure 5. Figure showing the flipping of the platelet due to interaction with high shear rate flow.

The flow velocity in the x -direction is given by the following equation

$$v_x = \zeta y + v_0, \quad (3.1)$$

where ζ is the shear rate and y is the y -coordinate of the SCE. In our simulations we set $\zeta = 10^{-3} \mu\text{s}^{-1}$, with offset velocity of $v_0 = 1.25 \times 10^{-5} \mu\text{m}/\mu\text{s}$. These parameters were obtained from (Mody & King 2005).

In our simulations, the relative platelet height H of the platelet from the vessel wall is selected as $H > 20$, where the units are multiples of the platelet radius r . Again this parameter is taken from (Mody & King 2005).

For the platelet parameters we use inter-SCE spring constant $\kappa_{\text{SCE}} = 2.4 \text{ fJ}/\mu\text{m}^2$ with all SCE connected to their nearest neighbors and the central SCE. This parameter is chosen from (Jadhav *et al* 2005) where the cell membrane elasticity is given as $0.3 - 3.0 \text{ fJ}/\mu\text{m}^2$.

The mass of each SCE is 0.08 pg by calculating the volume of the spheroid and assuming that the platelet has the same density as water. The platelet is constructed from SCE on the circumference of 5 circles stacked in the z -plane. The central (largest) circle we denote type 'circle 1', the adjacent two circles (above and below) we denote as type 'circle 2' and the remaining two (smallest) circles type 'circle 3'.

Article submitted to Royal Society

16 Christopher R. Sweet^{a,c,†}, Santanu Chatterjee^b, Zhiliang Xu^a, Katharine Bisordi^d, Elliot D. Rosen^d, Mark Alber^{a,†}

The effective radius of the SCE is $0.3 \mu\text{m}$ for ‘circle 3’, $0.2 \mu\text{m}$ for ‘circle 2’ and $0.1 \mu\text{m}$ for ‘circle 1’ (the largest radius circle) to provide a connecting surface map. We use a total of 53 SCEs with platelet $\lambda = 0.25$ (ratio of minor to major axis) as depicted in Figure 6.



Figure 6. Platelet constructed from 53 SCE.

To estimate the damping coefficient γ we consider the force from Stokes’ equation weighted by the mass, for a sphere it is

$$\gamma = \frac{6\pi\eta r}{m_i}, \quad (3.2)$$

where η is the viscosity of the fluid, set to $\eta = 1.2 \text{ nN}\mu\text{s}/\mu\text{s}^2$, r is the radius of the cell and m_i is the SCE mass. This yields an approximate figure of $283 \mu\text{s}^{-1}$, however the actual figure should be less since $\lambda < 1$.

We incorporate the adhesivity submodel described in Section iii (including the repulsive force) to constrain platelets within the simulated blood vessel and to account for the platelet-vessel wall interactions. We note that we do not provide simulations that specifically test this part of the model, but for completeness we use the estimated parameters from the literature. For the vessel wall we select the effective surface distance $\sigma = 0.45 \mu\text{m}$ from (Jadhav *et al* 2005), which is the combined receptor-ligand length. An estimate for cell-vessel adhesion coefficient can be made from (Jadhav *et al* 2005) as follows. If we consider that the rest length of the receptor-ligand is $0.45 \mu\text{m}$ and calculate the forward rate constants near to equilibrium, we have $k_r \approx 10^{-3} \mu\text{s}^{-1}$. The probability of bond rupture is $P_r = 1 - \exp(-k_r \delta t)$ for time δt , so by choosing a significant probability, say 0.5, we find that the bond lifetime is of the order of $1 \mu\text{s}$. If we further assume that the velocity of the cell is approximately equal to that of the liquid at a height of $3r$ then the ligand-receptor extension is $2 \times 10^{-3} \mu\text{m}$. From Section iii this gives adhesion coefficient $\epsilon = 8 \times 10^{-6} \text{ fJ}$ per receptor-ligand. From (Jadhav *et al* 2005) if we assume that there are of the order of 250 receptors per cell and 2 SCE contact the vessel, then we potentially have 6 bonds, equating to a combined adhesion coefficient $\epsilon_{\text{TOT}} = 5 \times 10^{-5} \text{ fJ}$. Note that the coefficients are combined as $\epsilon_{\text{TOT}} = \sqrt{\epsilon_{\text{SCE}} \epsilon_V}$ for the SCE and vessel coefficients respectively.

Note that all of the parameters used in the model are estimated from measurements from physical systems, there are no free parameters, see Table 2.

Article submitted to Royal Society

Table 2. Model parameters

Parameter	Value	Units	Reference
Shear rate ζ	10^{-3}	μs^{-1}	(Mody & King 2005)
κ_{SCE}	2.4	fJ/ μm^2	(Jadhav <i>et al</i> 2005)
SCE mass	0.08	pg	water density
SCE radius	0.1-0.3	μm	(Mody & King 2005)
SCE number	53		
λ	0.25	ratio	(Mody & King 2005)
ϵ_{TOT}	5×10^{-5}	fJ	(Jadhav <i>et al</i> 2005)
γ	283	μs^{-1}	

(ii) Platelet surface interaction with flow modification (SIM)

As discussed in Section vii, the Langevin-Stokes (LS) coupling does not take account of the cellular surface. Instead, each SCE is treated as if it is immersed in the fluid. We find that a more realistic description of the interaction can be achieved by treating the damping factor γ as if scaled along the vector connecting the surface SCE to the SCE at the platelet center. This effectively allows each SCE to “shield” other SCEs from the fluid flow field, as which would occur in a real flow scenario. In addition to this modification, the center SCE should see no effect from the flow. In the following text we refer to this as the Surface interaction modification (SIM) method.

In the first set of simulations for the platelet flipping, we employed both the basic LS coupling and the SIM method, where we effectively apply a local damping factor to each SCE. All simulation results are compared to the modified Jeffery orbit from (Mody *et al.* 2005a). In the LS model we expect the rate of initial rotation of the platelet to be larger since the flow interacts with all of the SCEs equally. With the SIM method the flow only acts on the surface SCEs facing the up-stream flow, which slows the initial rotation. These results are illustrated in Figure 7, where the advantages of utilizing the SIM approach can be clearly seen. The initial flow/platelet interaction follows the theoretical curve closely, in contrast to the basic LS approach.

(iii) The effect of the damping factor γ

In general the damping factor $\hat{\gamma}$ is chosen to model the viscosity of the fluid from Stokes’ law

$$\hat{\gamma} = 6\pi\eta r, \quad (3.3)$$

where η is the viscosity of the fluid and r is the radius of the spherical body. For our Langevin-Stokes approach, where we require that the fluid also acts as heat bath for our platelets, the actual value is divided by the mass of the SCE to give γ for our Langevin Equation (3.2) in Section B.1 of Supplementary Material. In addition the use of the SIM method means that the final value will be dependent on the geometry chosen for the platelet.

To determine the correct value we simulated the flipping platelet with a range of damping factors $25 \leq \gamma \leq 500$. The effect of changing this parameter can be seen in Figure 8, in which we also compared to the results of (G. B. Jeffery 1922). Optimal results occur at $\gamma = 250 \mu\text{s}^{-1}$ which is close to our estimated value of $283 \mu\text{s}^{-1}$ for a spherical cell.

18 Christopher R. Sweet^{a,c,†}, Santanu Chatterjee^b, Zhiliang Xu^a, Katharine Bisordi^d, Elliot D. Rosen^d, Mark Alber^{a,†}

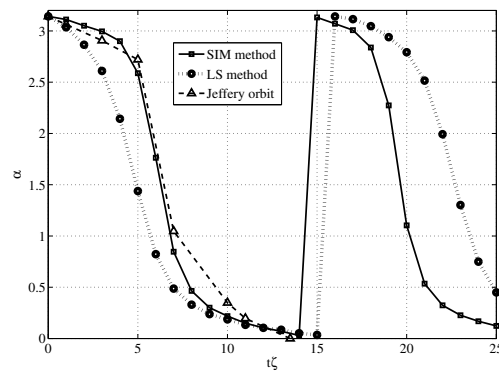


Figure 7. Comparison of the SIM and LS methods on the platelet flipping dynamics. The surface interaction method SIM shows flipping rates closer to the theoretical Jeffery orbit. The variation in angle α to the platelet major axis is plotted against the unit-less time, shear-rate product $t\dot{\gamma}$.

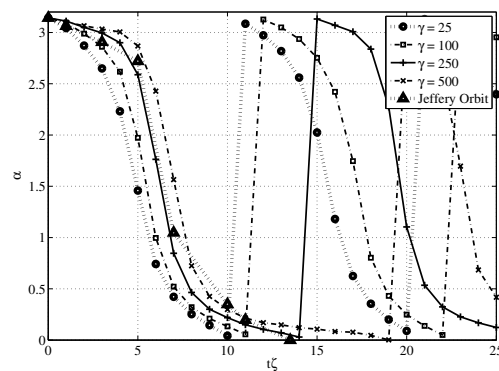


Figure 8. Effect of varying damping factor γ on the platelet flipping dynamics. The predicted value of $\gamma = 250$ shows flipping rates close to the theoretical Jeffery orbit. The variation in angle α to the platelet major axis is plotted against the unit-less time, shear-rate product $t\dot{\gamma}$.

(c) Stiffness of Platelet

Elasticity of the platelet is defined by the spring constant κ_{SCE} between pairs of SCEs in a cell. In our model, κ_{SCE} is not a free parameter as discussed above. Instead it is determined from experimental results, see Table 2. In this subsection, we demonstrate how the values of κ_{SCE} affect flipping dynamics of the platelet. The results can be seen in Figure 9. Here we ran simulations with $\kappa = 2.4, 10.0, 25.0, 50.0$ respectively. In each of these simulations we used $\gamma = 250.0 \mu s^{-1}$. It is evident that if the cell is less elastic, it flips faster under the influence of shear flow. Clearly, if the cell is more elastic, it can absorb more of the stress due to the flow.

In the paper (Mody & King et al. 2005a), simulations were used to characterize

Article submitted to Royal Society

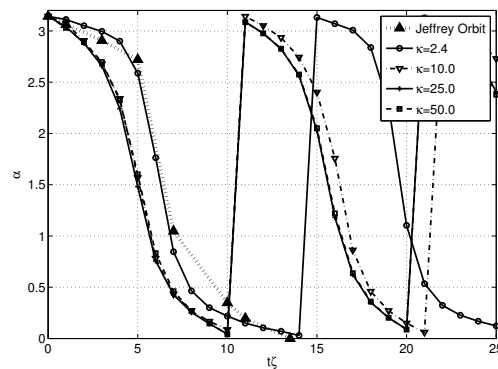


Figure 9. Effect of varying κ_{SCE} on the platelet flipping dynamics. As the stiffness of the platelets κ_{SCE} is increased the flipping rates become faster than the theoretical Jeffrey orbit. The variation in angle α to the platelet major axis is plotted against the unit-less time, shear-rate product $t\dot{\gamma}$.

trajectories of the freely flowing platelets. It was shown that platelets consistently attach to an adhesive surface only during the first-half of their rotation. Namely, angular orientations of platelets result in compression along the length of the platelet by the hydrodynamic flow forces. Our results suggest that the patterns of platelets flipping are also influenced by the mechanical properties of the platelet itself, which can subsequently affect the platelet binding to an adhesive surface. Conceivably, with a less elastic cell which flips faster, the time it remains in an orientation relative to the surface that permits binding, may be shorter than the time required for bond formation. On the other hand, a more elastic cell could stay in the orientation which allows to form the binding bond for a longer period of time once the cell makes the contact with the surface. Since experimental measurements of the effects of elasticity on platelet dynamics are not available at this time, we utilize simulations to predict the effects of the elasticity on the platelet flipping in the flow. The study of effect of platelet elasticity on binding to the surface will be the focus of the future work.

4. Discussion

The formation of intravascular thrombi can impair blood flow leading to ischemic damage to tissues in the vascular field of the vessel. A critical process in the formation or growth of a thrombus is the binding of resting platelets in the flowing blood with the injury site or developing thrombus surface. The binding of platelets is a multistep process involving the establishment of rapidly forming but transient interactions which slow the platelet and cause it to flip. The flipping on the thrombus or injury surface allows for the establishment of slower forming but stable adhesive bonds. To understand the recruitment of resting platelets it is necessary to understand the initial interactions which are governed by the blood flow, the orientation of the resting platelet flowing in blood and the mechanical properties of platelets.

The main focus of this paper is to describe and to demonstrate a new SCEL

Article submitted to Royal Society

20 Christopher R. Sweet^{a,c,†}, Santanu Chatterjee^b, Zhiliang Xu^a, Katharine Bisordi^d, Elliot D. Rosen^d, Mark Alber^{a,†}

method that couples continuum blood flow field, either fixed or modeled using an incompressible Navier-Stokes fluid solver, and discrete subcellular elements (SCE) model of a platelet using an innovative Langevin coupling approach. This is a *forward* coupling where the SCE dynamics are coupled to the flow field, but the flow calculations are not influenced by the SCE positions and velocities (see also Figure 10). It is shown that such coupling gives good agreement between simulation results and experimental data provided that the flow rate is not very high. In addition, a surface interface modification is introduced that more accurately models the fluid/platelet interface by considering the interaction to occur at the platelet surface. Moreover, since we utilize potentials to represent interactions among subcellular elements, we have further refined the basic adhesion models of (Sandersius & Newman 2008, Newman 2007) which utilizes potential energy to model adhesion, to both prevent cellular overlap and allow accurate representations of “flipping” dynamics of platelets. We would also like to point out that stochastic approach to model adhesion is better (Jadhav *et al.* 2005, Krasik *et al.* 2006, Mody & King 2008b), we will incorporate this approach in the future.

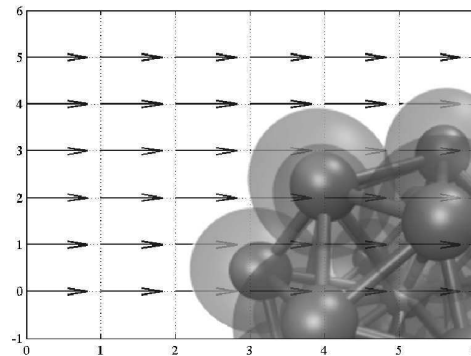


Figure 10. Forward flow coupling.

The extension of the SCE method (Newman 2007) described in this paper, allows modeling of platelet with realistic shape, elasticity and adhesivity coupled to the flow that is essential to the delivery mechanism in thrombus development in a blood vessel.

Using The SCEL, the 3D motion of a viscoelastic platelet in a shear blood flow was simulated and compared with experiments on tracking platelets in a blood flow chamber under conditions similar to those found in veins in terms of flow velocity and geometry. It has been shown that the complex platelet flipping dynamics under linear shear flows could be accurately recovered with the SCEL model when compared to the experiments. Simulation results in (Mody & King *et al.* 2005), in which platelets are represented as rigid ellipsoids, suggest that the patterns of platelet binding to and releasing from an adhesive surface are determined by hydrodynamic forces exerted on platelets. Because of this, binding bonds form only in specific platelet orientations where a hydrodynamic compressive force pushes the platelet against the surface. Our study suggests that platelet flipping is also influenced by

Article submitted to Royal Society

the mechanical properties of platelets. We show that a softer cell has a longer period of flipping in a blood flow. How cell elasticity affects platelet binding to the adhesive surface will be the subject of the future study.

5. Acknowledgments

This research was supported in part by NSF grant DMS-0800612, NIH grant HL073750-01A1 and the INGEN Initiative to Indiana University School of Medicine. We thank Timur Kupaev for the help with the image analysis of experimental data.

For Review Only

Article submitted to Royal Society

22 Christopher R. Sweet^{a,c,†}, Santanu Chatterjee^b, Zhiliang Xu^a, Katharine Bisordi^d, Elliot D. Rosen^d, Mark Alber^{a,†}

References

- Anderson, A., Chaplain, M. & Rejniak, K. 2007 Single-cell-based models in biology and medicine. *Mathematics and Biosciences in Inter- action*.
- Bunger, A., Brooks, C. & Karplus, M. 1984 Stochastic boundary conditions for molecular dynamics simulations of st2 water. *Chem. Phys. Let.*, **105**, 495–503.
- Christley, C., Lee, B., Dai, X. & Nie, Q. 2010, Integrative multicellular biological modeling: a case study of 3D epidermal development using GPU algorithms. *BMC Systems Biology*, **4**:107.
- Cruz, M., Diacovo, T., Emsley, J., Liddington, R. & Handin, R. 2000 Mapping the glycoprotein ib-binding site in the von willebrand factor a1 domain. *J. Biol. Chem.*, **275**, 252–255.
- Dopheide, S., Maxwell, M. & Jackson, S. 2002 Shear-dependent tether formation during platelet translocation on von willebrand factor. *Hemostasis, Thrombosis and Vascular Biology*, **99**, 159–167.
- Dembo, M. 1994 On peeling an adherent cell from a surface. In *Vol. 24 of series: Lectures on Mathematics in the Life Sciences, Some Mathematical Problems in Biology*. American Mathematical Society, Providence, RI. 51C77.
- Fogelson, A. & Guy, R. 2004 Platelet-wall interactions in continuum models of platelet aggregation: Formulation and numerical solution. *Mathematical Medicine and Biology*, **21**, 293–334.
- Fogelson, A. & Guy, R. 2008 Immersed-boundary-type models of intravascular platelet aggregation. *Computer Methods in Applied Mechanics and Engineering*, **197(25–28)**, 2087–2104.
- Frojmovic, M., Nash, G. & Diamond, S. 2002 Cell aggregation and cell adhesion in flow. *Thromb. Haem*, **87**, 771.
- Frenkel, D., & Smit, B. 2002 Understanding Molecular Simulation: From Algorithms to Applications, 2nd edition. *Academic Press*, ISBN: 0122673514.
- Gardiner, C.W., 2004, Handbook of Stochastic Methods. *Springer Series in Synergetics*, pp. 6–7. ISBN: 3-540-20882-8.
- Hansen, J. P. & McDonald, I. R. 1986 Theory of simple liquids. *Academic Press*.
- Heit, J., Cohen, A. & Anderson, F. J. 2005 Estimated annual number of incident and recurrent, non-fatal and fatal venous thromboembolism (VTE) events in the US. *Blood*, **106**, 267A.
- Izaguirre, J., Sweet, C. & Pande, V. 2010 Multiscale dynamics of macromolecules using normal mode langevin. *Pac. Symp. Biocomput.*, pp. 240–51.
- Jadhav, S., Eggleton, C. & Konstantopoulos, K. 2005 A 3-d computational model predicts that cell deformation affects selectin-mediated leukocyte rolling. *Biophysical J.*, **88**, 96–104.
- Jeffery, G. B. 1922 The motion of ellipsoidal particles immersed in a viscous fluid. *Proc. R. Soc. London, Ser. A* **102**, 161–167.
- Kasirer-Friede, A., Cozzi, M. R., Mazzucato, M., Marco, L. D., Ruggeri, Z. M. & Shattil, S. J. 2004 Signaling through gp ib-ix-v activates a iib b3 independently of other receptors. *Blood*, **103**, 3403–3411.
- King, M.R., Hammer, D.A. 2001, Multiparticle adhesive dynamics. Interactions between stably rolling cells. *Biophysical J.*, **81**:799-813.
- King, M.R. 2007, Influence of Brownian Motion on Blood Platelet Behavior and Adhesive Dynamics near a Planar Wall. *Langmuir*, **23(11)**:6321-6328.
- Kojic, M., Filipovic, N. & Tsuda, A. 2008 A mesoscopic bridging scale method for fluids and coupling dissipative particle dynamics with continuum finite element method. *Comput. Methods Appl. Mech. Engrg.*, **197**, 821833.

Article submitted to Royal Society

- 1
2
3
4 Krasik, E., Yee, K. & Hammer, D. 2006 Simulation of neutrophil arrest with deterministic
5 activation. *Biophysical J.*, **91**, 1145–1155.
- 6 Laurence, M. & Springer, T. 1991 Leukocyte roll on a selectin at physiologic flow rates:
7 distinction from and prerequisite for adhesion through integrins. *Cell*, **65**, 859–873.
- 8 Lennard-Jones, J. 1924 On the determination of molecular fields. *Proc. R. Soc. Lond. A*,
9 **106(738)**, 463–477.
- 10 Liu, W. K., Liu, Y., Farrell, D., Zhang, L., Wang, X. S., Fukui, Y., Patankar, N., Zhang, Y.,
11 Bajaj, C. *et al.* 2006 Immersed finite element method and its applications to biological
12 systems. *Comput. Methods Appl. Mech. Engrg.*, **195**, 1722–1749.
- 13 Meurer, R., Forrest, M., Springer, T. & Macintyre, D. 1999 The effects of ib4, a mono-
14 clonal antibody to the cd18 leukocyte integrin on phorbol myristate acetate (pma)-
15 induced polymorphonuclear leukocyte (pmn) accumulation and endothelial injury in
16 rabbit lungs. *Cell-Inflammation*, **23**, 51–62.
- 17 Mody, N.A., Lomakin, O., Doggett, T.A., Diacovo, T.G.; King, M.R. 2005a, Mechanics
18 of Transient Platelet Adhesion to von Willebrand Factor under flow. *Biophysical J.*,
19 **88:1432-1443**.
- 20 Mody, N. & King, M. 2005b Three-dimensional simulations of a platelet-shaped spheroid
21 near a wall in shear flow. *Phys. Fluids*, **17**.
- 22 Mody, N. & King, M. 2008a Platelet adhesive dynamics. part i: Characterization of platelet
23 hydrodynamic collisions and wall effects. *Biophysical J.*, **95**, 2539–2555.
- 24 Mody, N. & King, M. 2008b Platelet adhesive dynamics. part ii: High shear-induced tran-
25 sient aggregation via gpIb α -vWf-gpIb α bridging. *Biophysical J.*, **95**, 2556–2574.
- 26 Mu, J., Liu, X., Kamocka, M., Xu, Z., Alber, M., Rosen, E. & Chen, D.
27 2010 Segmentation, reconstruction, and analysis of blood thrombi in 2-photon mi-
28 croscopy images. *EURASIP Journal on Advances in Signal Processing*, p. 147216.
29 Doi:10.1155/2010/147216.
- 30 Mu, J., Liu, X., Kamocka, M., Xu, Z., Alber, M., Rosen, E. & Chen, D. 2009 Seg-
31 mentation, reconstruction, and analysis of blood thrombi in 2-photon microscopy im-
32 ages. *Proceedings of the 22nd IEEE Symposium on Computer-Based Medical Systems*
33 *(CBMS), Albuquerque, New Mexico, IEEE Xplore*, pp. 1–8. ISBN: 978-1-4244-4879-1,
34 doi: 10.1109/CBMS.2009.5255347.
- 35 Newman, T. 2007 Modeling multicellular structures using the subcellular element model.
36 *Single Cell Based Models in Biology and Medicine ed A Anderson, M Chaplain and K*
37 *Rejniak*, (Basle: Birkhäuser), 221–239.
- 38 Newman, T. 2008 Grid-free models of multicellular systems, with an application to large-
39 scale vortices accompanying primitive streak formation. *Current Topics in Develop-*
40 *mental Biology*, **81**, 157–182.
- 41 Pivkin, I. & Karniadakis, G. 2008 Accurate coarse-grained modeling of red blood cells.
42 *Physical Review Letters*, **101**, 118–105.
- 43 Rugger, Z. 1997 von willebrand factor. *J. Clin Invest.*, **99**, 559–564.
- 44 Sandersius, S. & Newman, T. 2008 Modeling cell rheology with the subcellular element
45 model. *Phys. Biol.*, **5**.
- 46 Savage, B., Saldivar, E. & Rugeri, Z. 1996 Initiation of platelet adhesion by arrest onto
47 fibrinogen or translocation on von willebrand factor (vWf). *Cell*, **84**, 289–297.
- 48 Skeel, R. & Izaguirre, J. 2002 An impulse integrator for langevin dynamics. *Mol. Phys.*,
49 **100**, 3885–3891.
- 50 Stalker, T., Wu, J., Morgans, A., Traxler, E., Wang, L., Chatterjee, M., Lee, D., Quarter-
51 mous, T., Hall, R. *et al.* 2009 Endothelial cell specific adhesion molecule (esam) local-
52 izes to platelet-platelet contacts and regulates thrombus formation in vivo. *J Thromb*
53 *Haemost.*, **7(11)**, 1886–1896.

54
55
56
57
58
59
60
Article submitted to Royal Society

1 24 Christopher R. Sweet^{a,c,†}, Santanu Chatterjee^b, Zhiliang Xu^a, Katharine Bisordi^d, Elliot D. Rosen^d, Mark Alber^{a,†}

2
3
4 Sweet, C., Petrone, P., Pande, V. & Izaguirre, J. 2008 Normal mode partitioning of
5 langevin dynamics for biomolecules. *J. Chem. Phys.*, **11**, 1–14.

6 Tandon, P. & Diamond, S. 1997 Hydrodynamic effects and receptor interactions of platelets
7 and their aggregates in linear shear flow. *Biophysical J.*, **73**, 2819.

8 Wakefield, T. W., McLafferty, R. B., Lohr, J. M., Caprini, J. A., Gillespie, D. L. & Pass-
9 man, M. A. 2009 Call to action to prevent venous thromboembolism. *J. Vasc. Surg.*,
10 **49**(6), 1620–1623.

11 Xu, Z., Chen, N., Kamocka, M., Rosen, E. & Alber, M. 2008 Multiscale model of thrombus
12 development. *Journal of the Royal Society Interface*, **5**, 705–722.

13 Xu, Z., Chen, N., Shadden, S., Marsden, J., Kamocka, M., Rosen, E. & Alber, M. 2009a
14 Study of blood flow effects on growth of thrombi using a multiscale model. *Soft Matter*,
15 **5**, 769–779.

16 Xu, Z., Lioi, J., Mu, J., Kamocka, M., Liu, X., Chen, D., Rosen, E. & Alber, M. 2010 A
17 multiscale model of venous thrombus formation with surface-mediated control of blood
18 coagulation cascade. *Biophysical Journal*, **98**(9), 1723–1732.

19 Xu, Z., Mu, J., Liu, X., Kamocka, M., Rosen, E., Chen, D. & Alber, M. 2009b Com-
20 bined experimental and simulation study of blood clot formation. *Proceedings of the*
21 *2009 IEEE Toronto International Conference - Science and Technology for Human-*
22 *ity TIC-STH, Toronto, Canada, IEEE Xplore*, pp. 357–362. ISBN: 978-1-4244-3878-5,
23 doi:10.1109/TIC-STH.2009.5444476.

24
25
26
27
28
29
30
31
32
33
34
35
36
37
38
39
40
41
42
43
44
45
46
47
48
49
50
51
52 Article submitted to Royal Society
53
54
55
56
57
58
59
60